CD81 is essential for the formation of membrane protrusions and regulates Rac1-activation in adhesion-dependent immune cell migration

Thomas Quast,[1] Felix Eppler,[1] Verena Semmling,[2] Cora Schild,[1] Yahya Homsi,[3] Shoshana Levy,[4] Thorsten Lang,[3] Christian Kurts,[2] and Waldemar Kolanus[1]

[1]Laboratory of Molecular Immunology, Life and Medical Sciences (LIMES) Institute, University of Bonn, Bonn, Germany; [2]Institute of Experimental Immunology, University of Bonn, Bonn, Germany; [3]Laboratory of Membrane Biochemistry, LIMES Institute, University of Bonn, Bonn, Germany; and [4]Department of Medicine, Division of Oncology, Stanford University Medical Center, Stanford, CA

CD81 (TAPA-1) is a member of the widely expressed and evolutionary conserved tetraspanin family that forms complexes with a variety of other cell surface receptors and facilitates hepatitis C virus entry. Here, we show that CD81 is specifically required for the formation of lamellipodia in migrating dendritic cells (DCs). Mouse *CD81*$^{-/-}$ DCs, or murine and human CD81 RNA interference knockdown DCs lacked the ability to form actin protrusions, thereby impairing their motility dramatically. Moreover, we observed a selective loss of Rac1 activity in the absence of CD81, the latter of which is exclusively required for integrin-dependent migration on 2-dimensional substrates. Neither integrin affinity for substrate nor the size of basal integrin clusters was affected by CD81 deficiency in adherent DCs. However, the use of total internal reflection fluorescence microscopy revealed an accumulation of integrin clusters above the basal layer in CD81 knockdown cells. Furthermore, β1- or β2-integrins, actin, and Rac are strongly colocalized at the leading edge of DCs, but the very fronts of these cells protrude CD81-containing membranes that project outward from the actin–integrin area. Taken together, these data suggest a thus far unappreciated role for CD81 in the mobilization of preformed integrin clusters into the leading edge of migratory DCs on 2-dimensional surfaces. (*Blood*. 2011;118(7):1818-1827)

Introduction

CD81 (TAPA-1) is a member of the tetraspanin family, a large group of evolutionary conserved membrane proteins containing 4 transmembrane domains.[1] The most distinctive feature of the tetraspanin proteins is the ability to form lateral associations with one another and to cluster dynamically with multiple cell surface receptors.[2-5] Tetraspanins are capable of recruiting specific intracellular signaling enzymes, including protein kinase C,[3] that is known to be involved in integrin phosphorylation. In *CD81*$^{-/-}$ mice, sperm–egg fusion is reduced during oocyte fertilization,[6] and antibody-mediated immune responses are significantly delayed.[7] On B cells, CD81 is required for molecular organization and efficient collaboration between the B-cell receptor and CD21, CD19, and various signaling enzymes.[5] CD81 is required for maturation and surface expression of CD19, a molecule with a key role during B-cell activation.[8]

Importantly, CD81 associates with the $\alpha_4\beta_1$-integrin on B cells[9] and has been reported to interface between the plasma membrane and the cytoskeleton in B cells by mobilizing ezrin.[10] On T cells and on antigen-presenting cells, CD81 distributes into immune synapses.[11] Like other tetraspanins, CD81 is involved at multiple steps in both HIV-1[12] and hepatitis C virus infection.[13]

Persistent migration requires multiple cellular changes involving polarization of the microtubular cytoskeleton and the secretory pathway.[14] In contrast to the well understood cell migration mechanisms of slow-moving cells, for example, fibroblasts and epithelial cells, the migration mode of leukocytes seems complex and depends on various environmental conditions. Extravasation of leukocytes requires integrin-dependent cell adhesion and proteolysis of extracellular matrix (ECM) in combination with fundamental shape changes of the cell body.[15] Alternatively, interstitial migration of leukocytes inside tissues was shown to be independent of proteolysis and is characterized by only marginal interactions of the cells with constituents of the ECM.[16,17] Recent studies postulate that leukocyte migration inside a 3-dimensional collagen gel is independent of integrin-mediated adhesion in vitro and partially integrin-dependent in vivo.[18,19] Subsequently, we showed that immune cell migration might be subclassified into an integrin-dependent and an integrin-independent mode.[20] The latter migration mode is characterized by high plasticity of the cell body and fast alternating cycles of morphologic expansion and contraction, which is based on a highly dynamic actin cytoskeleton.[19,20] Interactions of leukocytes with the ECM are mediated by fast aggregation of membrane receptors because of the lack of focal contacts and stress fibers (reviewed in Friedl et al[21]).

Models that were based on studies using slow-moving fibroblasts and epithelial cells proposed a strongly coordinated 4-step process consisting of actin-dependent membrane protrusion formation at the leading edge, adhesion to the substratum, retraction, and de-adhesion of the cell rear.[22] The signals for the initialization of actin assembly are provided by constituents of the ECM, such as fibronectin and collagen, via integrin signal transduction and by soluble motogens, such as chemokines and growth factors. They initiate activation of the small GTPases of the Rho family (Rac1,

Submitted December 21, 2010; accepted June 1, 2011. Prepublished online as *Blood* First Edition paper, June 15, 2011; DOI 10.1182/blood-2010-12-326595.

The online version of the article contains a data supplement.

The publication costs of this article were defrayed in part by page charge payment. Therefore, and solely to indicate this fact, this article is hereby marked "advertisement" in accordance with 18 USC section 1734.

RhoA, and Cdc42) that play critical roles in signal transduction and actin cytoskeletal reorganization during lamellipodia formation.[23]

Notwithstanding previous reports on the molecular functions of tetraspanin proteins in regulating cell motility,[24,25] our understanding of the specific role of CD81 in immune cell migration has remained fragmentary. We show here that CD81 is essential for dendritic cell (DC) migration on 2-dimensional surfaces but not for their chemotaxis in 3-dimensional collagen. *CD81*$^{-/-}$ or knockdown cells from mice and humans displayed severely impaired actin protrusions at the cell front. They were also characterized by a strong defect in Rac signaling and did not migrate. These functional impairments are clearly linked to defects in cell adhesion, as is demonstrated both statically and by visualization of actin dynamics at the single cell level. Most significantly, CD81-deficient cells were capable of activating the high-affinity form of β1-integrins and the size of substrate-engaged integrin clusters also was found to be normal. In contrast, loss of CD81 expression resulted in a dramatic reduction of lamellipodial spreading and in the accumulation of preformed integrin clusters above the basal layer. Together with our discovery that the leading edge of adherent DCs bears a rim of CD81-containing membranes that lacks either integrins or actin, these data suggest a novel role of CD81 in the mobilization of integrin clusters into the outer edge of the protruding cell front.

Methods

Generation of murine BM-derived DCs

See supplemental Methods (available on the *Blood* Web site; see the Supplemental Materials link at the top of the online article).

Generation of human monocyte-derived DCs

See supplemental Methods.

Antibodies, inhibitor, qRT-PCR tubes, and compounds

The following antibodies were against the human antigens: HLA-DR (clone G 46-6), CD40 (clone 5C3), CD80 (clone 3H5), CD81 (clone JS-81), CD86 (clone 24F; all from BD Biosciences Pharmingen), CD29 (clone MEM-101A; ImmunoTools), and the active conformation of β1-integrin (clone HUTS-4; Millipore Bioscience Research Reagents). These antibodies were against the following mouse antigens: CD18 (clone M18/2; BioLegend), β1-integrin (clone 12G10; Millipore Bioscience Research Reagents), CD11c (clone 3.9), CD80 (clone 16-10A1), CD81 (clone EAT 2), CD9 (clone KMC8), CD86 (clone B7-2), MHCII (all from eBioscience), Talin1 (Abcam), and tubulin (Millipore Bioscience Research Reagents). This antibody was against both human and mouse antigen: actin (Sigma-Aldrich). For flow cytometric analysis, the following isotype-matched antibody controls were used: rat IgGI PE (BD Biosciences Pharmingen) and rat IgGI FITC (clone eBRG1; eBioscience). Cell permeable Rac1 inhibitor (NSC23766) was purchased from Calbiochem.

qPCR was performed with the following TaqMan probes (Applied Biosystems): Rac1 (Mm01201653_mH), Rac2 (Mm00485472_m1), and Rac3 (Mm00652427_g1). GAPDH probe (4352932E) was used as endogenous control. Phorbol-12-myristate-13-acetate (PMA) is a synthetic structural analog of diacylglycerol and was purchased from Sigma-Aldrich.

Oligonucleotide sequences and plasmids

RNA interference (RNAi) was performed using oligonucleotides against the following target sequences: CD81 (human), 5′-CCUUCUAUGUAGGCAUCUA-3′; CD81 (mouse), 5′-TACCTGGAACTGGGAAASAAA-3′; Rac2 (mouse), 5′-CTGGCCAAGGATATTGATTCA-3′; and Talin1 (mouse), 5′-TGGGAAAGCTTTGGACTACTA-3′; *Renilla* luciferase sequence was used as a control (5′-AAACAUGCAGAAAAUGCUG-3′).

All small-interfering RNAs (siRNAs) were purchased from QIAGEN or Dharmacon RNA Technologies, respectively. The overexpression constructs EGFP-Rac1-wildtype, EGFP-Rac1-Q61L, and EGFP-Rac1-T17N were purchased from Addgene. The overexpression construct Lifeact-enhanced green fluorescent protein (EGFP)[26] was provided by Peter Lipp (Institute for Molecular Cell Biology, Saarland University).

Transfection of siRNAs

Oligonucleotides were transferred to a 4-mm cuvette (Bridge) and incubated for 3 minutes with 4×10^6 immature dendritic cells in 100 μL Opti-MEM (Invitrogen) before electroporation in a Gene Pulser X cell + CE module (Bio-Rad Laboratories). Pulse conditions were square wave, 1000 V, 2 pulses, and 0.5-ms pulse length. Forty-eight hours after electroporation, immature dendritic cells were stimulated to mature (see supplemental Methods). Seventy-two to 120 hours after electroporation, RNAi efficiency was tested using flow cytometry, Western blotting or qRT-PCR, respectively.

Transfection of BM-DCs with plasmid DNA

Transfections of BM-DCs with plasmid DNA were carried out as described previously.[20] In brief, 1×10^5 mature BM-DCs were transfected with 4 μg of EGFP-plasmid DNA in 100 μL of Opti-MEM using the MicroPorator MP-100 system (DigitalBio). Pulse conditions were 1500 V, 30 ms, and 1 pulse. BM-DCs were used for functional assays 24 hours after transfection. The obtained transfection efficiency was ~ 10%.

In vitro analysis of chemotaxis in a 3-dimensional collagen gel

Three-dimensional chemotaxis assays were processed as described previously,[22,27] with the following modifications. Collagen I (Pure Col; Inamed) was mixed with 7.5% sodium bicarbonate (Invitrogen) and 10× MEM (Sigma-Aldrich) on ice. BM-DCs in VLE-RPMI 1640 and 0.5% FCS were carefully mixed with the collagen solution at a 2:1 ratio, resulting in gels with a collagen concentration of 1.6 mg/mL and a final cell concentration of 1.5×10^6 cells/mL gel. Collagen–BM-DC mixtures were carefully placed in custom-made chemotaxis chambers and incubated at 37°C and 5% CO_2 for 60 minutes. After collagen polymerization, 600 ng/mL CCL19 (R&D Systems or PeproTech) in VLE-RPMI 1640 and 0.5% FCS was added on top of the gel. Time-lapse series of motile BM-DCs in 3-dimensional collagen gel were recorded using a fully automated inverted TE Eclipse microscope (Nikon) equipped with a 10× phase contrast objective (Nikon), motorized xyz-stage (Märzhäuser), climate chamber (37°C, 5% CO_2, humidified) and a CCD-1300 camera (Vosskühler). Before analysis of chemotaxis parameters BM-DC were tracked over 3 hours (5 minutes/frame) using the manual tracking plugin of ImageJ. Subsequently cell velocity and y-Forward Migration Index (see above) were calculated using the Chemotaxis and Migration tool plugin (Ibidi) for Image J.

Static adhesion assay

See supplemental Methods.

Analysis of actin dynamics using an under-agarose chemotaxis assay

Because of low adhesion of LPS-stimulated BM-DC we visualized cortical actin flow under an agarose gel as described before[28,29] with the following modifications. Motile BM-DC were monitored using an inverted Zeiss 5 Live confocal microscope at 488-nm excitation wavelength equipped with a climate chamber (37°C, 5% CO_2, humidified) and a Plan-Fluar 100×/1.45 oil immersion Objective (Carl Zeiss). In these under-agarose assays, polarized BM-DCs showed a flat and expanding lamellipodium projected in 1 defined focus layer. Retrograde flow of F-actin was observed near the basal plasma membrane of Lifeact-EGFP–transfected BM-DCs. For the under-agarose assays, 2× HBSS buffer (Invitrogen), RPMI 1640 (PAA Laboratories) supplemented with 20% (vol/vol) heat-inactivated FCS (Sigma-Aldrich), and 3.5% agarose (Invitrogen) were mixed in a 1:2:1 ratio and subsequently casted into a fibronectin-coated (Harbor Bio-Products)

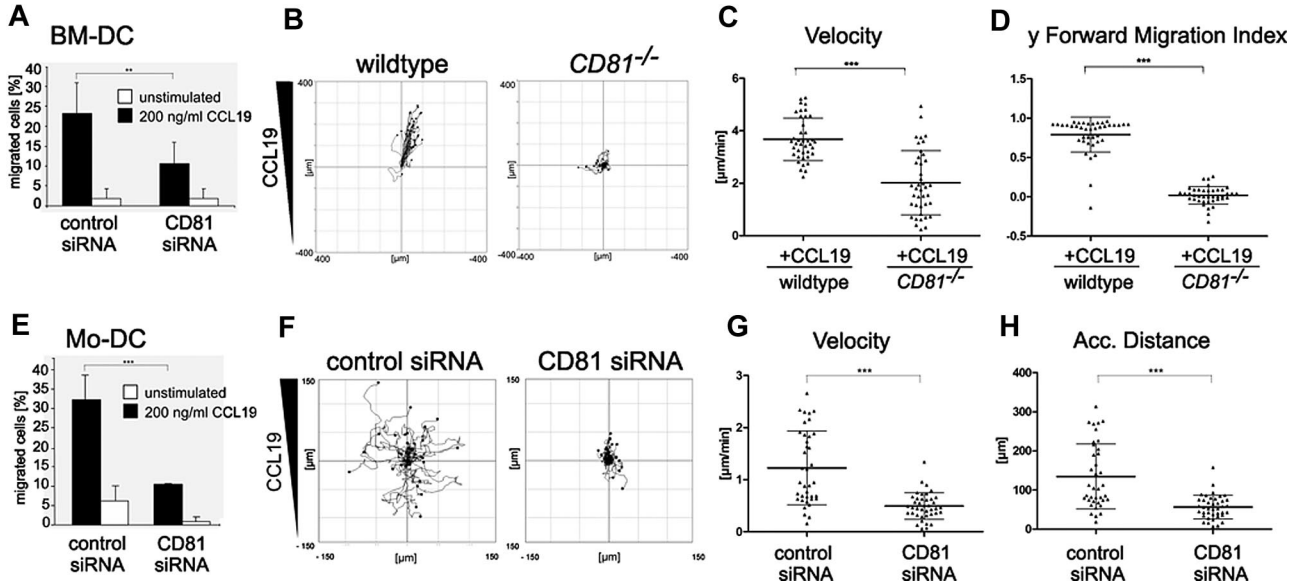

Figure 1. CD81 is important for chemotaxis of DCs on 2-dimensional substrates. Transwell migration assays of LPS-stimulated (200 ng/mL) CD81 RNAi knockdown BM-DCs (A) and CD81 RNAi knockdown Mo-DCs (E) toward CCL19 (200 ng/mL). Chemotactic migration of BM-DCs (B-D) and Mo-DCs (F-H) in response to a stable CCL19 gradient (200 ng/mL) on 2-dimensional fibronectin-coated (50 μg/mL) commercial chemotaxis chambers. Migration plots of 40 cells/sample monitored by time-lapse videomicroscopy over a period of 1 hour by capturing digital images every minute from 1 representative experiment of 3 are depicted (B,F). Quantification of average migratory speed (velocity; C,G), y-forward migration index (y-FMI, which means directional persistence toward the chemokine; D), and accumulated (Acc.) distance of migrating DCs (H) after manual tracking of motile cells are representative for 1 experiment of 3. Error bars indicate ± SD. $^{**}P \leq .01$, $^{***}P \leq .001$.

35 mm μ-dish (Ibidi); hardened at room temperature for 1 hour; and equilibrated at 37°C and 5% CO_2 for 30 minutes. Subsequently, a hole was stamped into the agarose gel and filled with 600 ng/mL CCL19 (PeproTech). Within a distance of 5 mm, 1×10^5 BM-DCs were injected between the bottom of the dish and the agarose gel. Time-lapse videomicroscopy was initiated when BM-DCs started to migrate toward the chemokine gradient. BM-DCs were generally tracked for at least 5 minutes at 2 seconds per frame. Velocities of both actin cortical flow and membrane protrusion were analyzed by kymograph and line-scan analysis after application of the walking average plug-in, using ImageJ 1.38x (National Institutes of Health; http://imagej.nih.gov/ij/). Actin polymerization rate was calculated as the sum of actin cortical flow and membrane protrusion.

TIRF microscopy

Total internal reflection fluorescence (TIRF) microscopy was performed as described previously.[30] In brief, a TIRF microscope (based on a motorized IX81 microscope; Olympus) equipped with an electron-multiplying charge-coupled device camera (ImagEM C9100-13; Hamamatsu Photonics), a 488 nm laser, and a 150-W xenon lamp integrated into the MT20-I fluorescence illumination system were used. Furthermore, a 60× NA 1.49 Apochromat objective in combination with a 2× and 1.6× magnifying lens was used. For TIRF illumination, we used the 488 nm laser line and the U-MTIR488-HC filter (Olympus). For epifluorescence, a xenon lamp together with the F36-525 EGFP HC-Filterset (AHF Analysentechnik) was used. The exposure time was 1 second for epifluorescence, 400 ms for TIRF, and the camera gain was set to 100. For image autocorrelation analysis, we used the ImageJ program. Squared regions of interest (ROIs) ranging from 20×20 to 50×50 pixels were placed either at the central or a peripheral area of the basal plasma membrane. The ROI was correlated with the original (yielding a correlation coefficient of 1), and then the original image was displaced pixel-wise up to 15 pixels. The correlation coefficient was determined after each displacement. Four values were averaged yielding an autocorrelation curve for the respective ROI. From individual cells, autocorrelation curves were averaged. Values are given as mean ± SD (n = 5 cells).

Statistical analysis

Statistical significance between data groups was determined by ANOVA or unpaired *t* test with Prism software (GraphPad Software) and considered to be significantly different at values of $P < .05$. The P values are depicted as asterisks in the figures as follows: $^{***}P < .001$, $^{**}P < .01$, and $^{*}P < .05$.

Image acquisition

See supplemental Methods.

Results

DC migration plays a key role in initiating immune responses, because DCs are the most important professional antigen-presenting cells. Migration of DCs into peripheral tissues and their emigration to draining lymph nodes after pathogen encounter are coordinated by multiple chemokine–chemokine receptor pairs. A large body of work showed that the chemokines CCL19 and CCL21 regulate inflammatory migration of DCs through binding to CCR7, which is strongly up-regulated during DC maturation.[31]

CD81 is not required for the maturation of DCs

To determine the role of CD81 in DC migration, we used murine CD81-null ($CD81^{-/-}$) DCs.[7] Western blot analysis showed that $CD81^{-/-}$ BM-DCs did not express any CD81 protein (supplemental Figure 1A). Because some tetraspanins have been described to be functionally overlapping,[32] we also performed CD81 RNAi knockdown analysis with wild-type DCs from mice or humans to exclude indirect compensatory effects of the loss of CD81 during murine development. At day 8 of culture, murine BM-DCs or human monocyte (Mo)–DCs were either used in the immature state, or they were matured by adding lipopolysaccharide (LPS) for 48 hours, respectively. Compared with DCs that had been transfected with control siRNA, RNAi of CD81 significantly reduced the specific protein expression in both BM-DCs and Mo-DCs, as detected by flow cytometry (supplemental Figure 1B,D). All cells showed normal surface expression of maturation markers, including costimulatory molecules and major histocompatibility complex

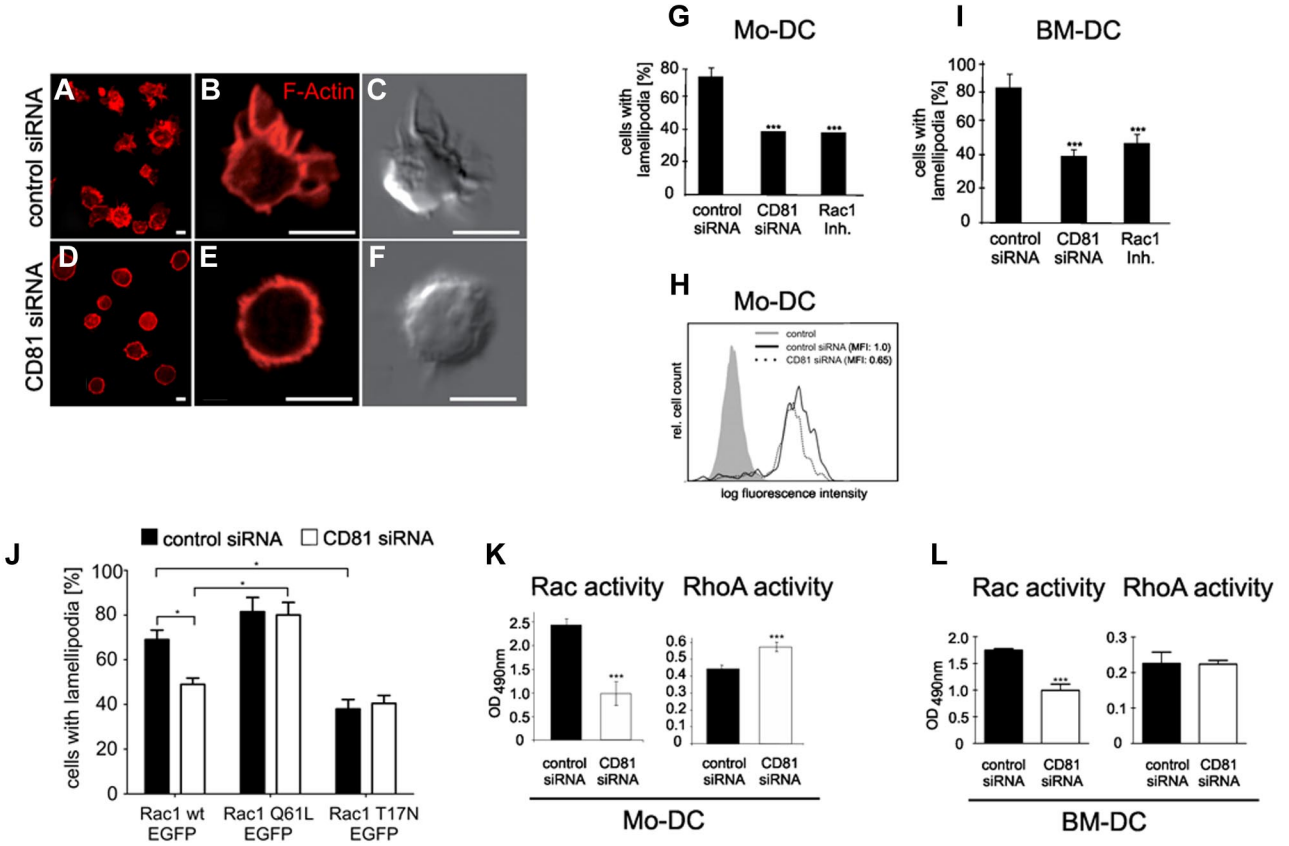

Figure 2. CD81 is important for the formation of Rac-dependent actin membrane protrusions. Microscopic visualization of F-actin by the use of Cy3-phalloidin in BM-DCs after transfection with control siRNA (A-B) or CD81 siRNA (D-E). Corresponding differential interference contrast images to panels B and E, respectively (C,F). Quantification of membrane protrusions in LPS-stimulated Mo-DCs (G) and BM-DCs (I-J) on 2-dimensional fibronectin-coated surfaces, respectively. Quantification of membrane protrusions after overexpression with wild-type Rac1, constitutive active or dominant-negative Rac1 mutant (Q61L and T17N, respectively), all linked to EGFP (J). In each individual experiment, 200 mature phalloidin-stained BM-DCs were counted by the use of fluorescence microscopy (G, I-J). Measurement of F-actin by flow cytometry after Alexa 488-phalloidin staining of LPS-stimulated Mo-DCs (H). Analysis of the basal activities (GTP loading) of the small GTPases Rac or RhoA after RNAi of CD81 using commercial enzyme-linked assay (K-L). All shown fluorescence staining images (A-B,D-E) are confocal images, focused to the basal plasma membrane of the respective cells. Bars represent 5 μm. Each single experiment was performed in duplicate. Each experiment was repeated at least 3 times independently. Error bars indicate ± SD. $*P \leq .05$, $***P \leq .001$.

(MHC) II (supplemental Figure 1C,E). These findings showed that DC maturation, a prerequisite of DC migration, is not compromised by the absence of CD81. Because it was reported that the tetraspanins CD81 and CD9 may have redundant functions, we analyzed protein expression levels of CD9 after RNAi of CD81. Expression levels of CD9 were not altered in CD81 RNAi knockdown DCs, as detected by flow cytometry (supplemental Figure 1C).

CD81 regulates migration of DCs on 2-dimensional surfaces in vitro

Maturation after antigen capture enables DCs to emigrate from the infected tissues and organs to draining lymph nodes, where they activate naive lymphocytes. To assess directional chemotaxis of DCs, we first performed modified Boyden chamber assays (so-called transwell migration assays). RNAi of CD81 strongly reduced CCL19-stimulated chemotaxis of LPS-matured BM-DCs (Figure 1A) or Mo-DCs (Figure 1E), compared with cells transfected with control siRNA.

Furthermore, by the use of time-lapse videomicroscopy and subsequent computer-assisted calculations, we confirmed that CD81 is required for CCL19-stimulated migration of both LPS-stimulated BM-DCs and Mo-DCs on 2-dimensional surfaces in vitro. The importance of CD81 as an endogenous regulator of DC motility was confirmed using CD81 knockout mice. Tracks of single cells visualized as plots show that CCL19-stimulated cell migration of *CD81*$^{-/-}$ BM-DCs on fibronectin-coated surfaces is strongly impaired compared with that of wild-type cells (Figure 1B; supplemental Videos 1-2). We detected that average velocity and y-forward migration index of *CD81*$^{-/-}$ BM-DCs were significantly reduced compared with those of control cells (Figure 1C-D). Furthermore, we analyzed migration parameters of human Mo-DCs. Because high directional persistence is generally difficult to obtain with human Mo-DCs, we only analyzed parameters of chemokinesis. Figure 1F and supplemental Videos 3 and 4 show that RNAi of CD81 strongly abrogates CCL19-stimulated migration of Mo-DCs on 2-dimensional fibronectin-coated surfaces and significantly reduces velocity (Figure 1G) and accumulated distance (Figure 1H) of motile cells. Taken together, these data provide strong evidence that the tetraspanin CD81 is an important regulator of DC migration on 2-dimensional substrates.

CD81 is required for the formation of actin membrane protrusions via Rac activation

Cell migration to chemoattractant gradients highly depends on the formation of membrane protrusions. These so-called lamellipodia are planar structures whose dynamics is based on coordinated alternating actin polymerization and depolymerization. Formation

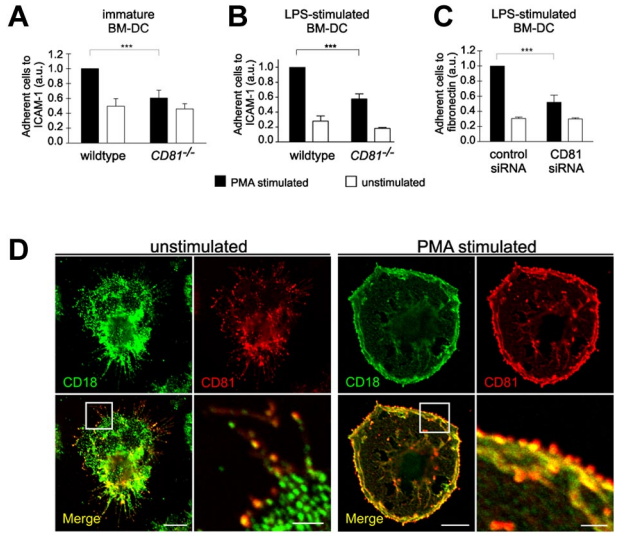

Figure 3. CD81 controls static integrin adhesion of DCs. Static adhesion of unstimulated immature BM-DCs (A) or of LPS-stimulated (200 ng/mL) BM-DCs (B-C) to surfaces coated with 12.5 μg/mL ICAM-1-FC (A-B) or 50 μg/mL fibronectin (C), respectively. BM-DCs were stimulated with 50 ng/mL PMA. Immunofluorescence stainings reveal that CD81 (red fluorescence) is colocalized with β2 integrins (CD18, green fluorescence) in migration-relevant membrane protrusions (D left panel). PMA stimulation leads to an increased relocalization and strong accumulation of colocalized CD81 and CD18 to the cell periphery at the leading edge of membrane protrusions (D right panel). Error bars indicate ± SD. ***$P \leq .001$. Each single experiment was performed in duplicate. Each experiment was repeated at least 3 times independently. Bars represent 10 and 2 μm (magnified detail), respectively.

of lamellipodia may be spontaneous, but it is also induced by chemokines or by bacterial and ECM degradation products. Lamellipodia are regulated by tight coordination of Rho GTPase activity.[33,34] Because CD81-deficient DC show strong defects in migration, we further analyzed whether actin cytoskeleton dynamics are affected by CD81. By the use of Cy3-phalloidin staining of formaldehyde-fixed mature Mo-DCs and BM-DCs, we found that the formation of actin-based membrane protrusions on fibronectin-coated surfaces is strongly impaired after RNAi of CD81 compared with that of mature DCs transfected with control siRNA; the latter cells show F-actin in broad membrane protrusions (Figure 2A-F and G,I). Quantification of cellular F-actin content by flow cytometry after Alexa 488–phalloidin staining of LPS-stimulated Mo-DCs revealed that RNAi of CD81 reduces actin polymerization, compared with that of control cells (Figure 2H). Interestingly, CD81 knockdown DCs show a morphologic phenotype comparable with DCs after specific inhibition of Rac1 activity (Figure 2G,I). Finally, overexpression analysis revealed that Rac1 function is required for the formation of lamellipodia in BM-DCs. To this end, we used the microporation system method[20] to overexpress EGFP-wild-type Rac1 or the EGFP-Rac1 mutants Q61L or T17N (Rac1 constitutively active or dominant negative, respectively). Figure 2J shows that overexpression of the Rac1-T17N mutant strongly reduced lamellipodia formation in BM-DCs compared with that in cells that had been transfected with EGFP-wild-type Rac1. RNAi of CD81 clearly reduced lamellipodia formation of BM-DCs only in cells that had been transfected with EGFP-wild-type Rac1, but not in cells transfected with the Rac1 mutant Q61L or T17N, respectively. We conclude from these results that CD81 is required upstream of Rac1 for the generation of actin membrane protrusions in this cell type. These findings prompted us to investigate into a possible role of CD81 in Rac activation. We observed that RNAi of CD81 strongly reduced GTP-loading of Rac in both Mo-DCs and BM-DCs, whereas the activity of RhoA was moderately enhanced in CD81 knockdown Mo-DCs or unaffected in CD81 knockdown BM-DCs compared with DCs that were transfected with control siRNA (Figure 2K-L). The apparent differences in RhoA activity in the murine and human cells, respectively, might be because of differences in RNAi efficiency in these cell types. Taken together, we conclude that CD81 acts upstream of Rac in mediating lamellipodia formation and directs DC migration on 2-dimensional substrates.

CD81 neither regulates β1-integrin affinity nor avidity, but it organizes integrin cluster distribution

Because cell migration on 2-dimensional substrates requires the binding of adhesion receptors to extracellular ligands, we further analyzed whether DC adhesion is affected by CD81. We therefore assessed static cell adhesion to ICAM-1 or fibronectin using *CD81*$^{-/-}$ or CD81 RNAi knockdown BM-DCs. Depletion of CD81 or RNAi of CD81 markedly reduced static adhesion of PMA-stimulated BM-DCs to ICAM-1 or fibronectin (Figure 3A-C). We suggest from these findings that CD81 is an important regulator of β2- and β1-integrin–mediated DC adhesion. These results were strongly supported by the colocalization of CD81 with both β2-integrins (CD18; Figure 3D) and β1-integrins (CD29; supplemental Figure 2B) in adhesion- and migration-relevant membrane protrusions of DCs. PMA stimulation leads to an increased relocalization and strong accumulation of colocalized CD81 and CD18 to the cell periphery at the leading edge of membrane protrusions (Figure 3D right panel).

To investigate into a possible upstream role of CD81 in regulating integrin activity, we analyzed expression levels as well as affinity and avidity of β1-integrins in LPS-stimulated Mo-DCs (Figure 4). Flow cytometric analysis shows that expression levels of constitutively expressed CD29 were not abrogated after RNAi of CD81 (Figure 4A left panel). Furthermore, PMA stimulation increases the expression of the high-affinity state of β1-integrins as detected by a monoclonal antibody (clone HUTS-4) directed against an activation epitope of CD29 (Figure 4A right panel). Because RNAi of CD81 does not abrogate PMA-stimulated activation of the activation epitope, we conclude that CD81 does not regulate β1-integrin affinity.

To investigate into a possible role of CD81 in integrin avidity regulation, we performed confocal laser scanning microscopy and conventional epifluorescence microscopy to analyze CD29 localization in the plasma membrane of nonpermeabilized Mo-DCs that were adherent to fibronectin-coated surfaces (Figure 4B-C). The fluorescence images show that in contrast to homogeneous localization of CD29 clusters in control DCs, RNAi of CD81 leads to an accumulation of CD29 in plasma membrane ruffles in the perinuclear cell region (Figure 4B right panel and 4C left panel). We performed TIRF microscopy to analyze integrin cluster size and avidity in the basal plasma membrane with a better axial resolution compared with conventional epifluorescence microscopy in which background fluorescence overwhelms the focus plane (Figure 4C). TIRF microscopy allows the selective illumination and excitation of fluorophores in a restricted region of the cells close to the glass–water interface. Subsequent autocorrelation analysis of the data showed that there were no significant differences in integrin-cluster size after RNAi of CD81 compared with wild-type control. Cluster size and distribution was not different in central regions compared with peripheral plasma membrane regions (Figure 4C).

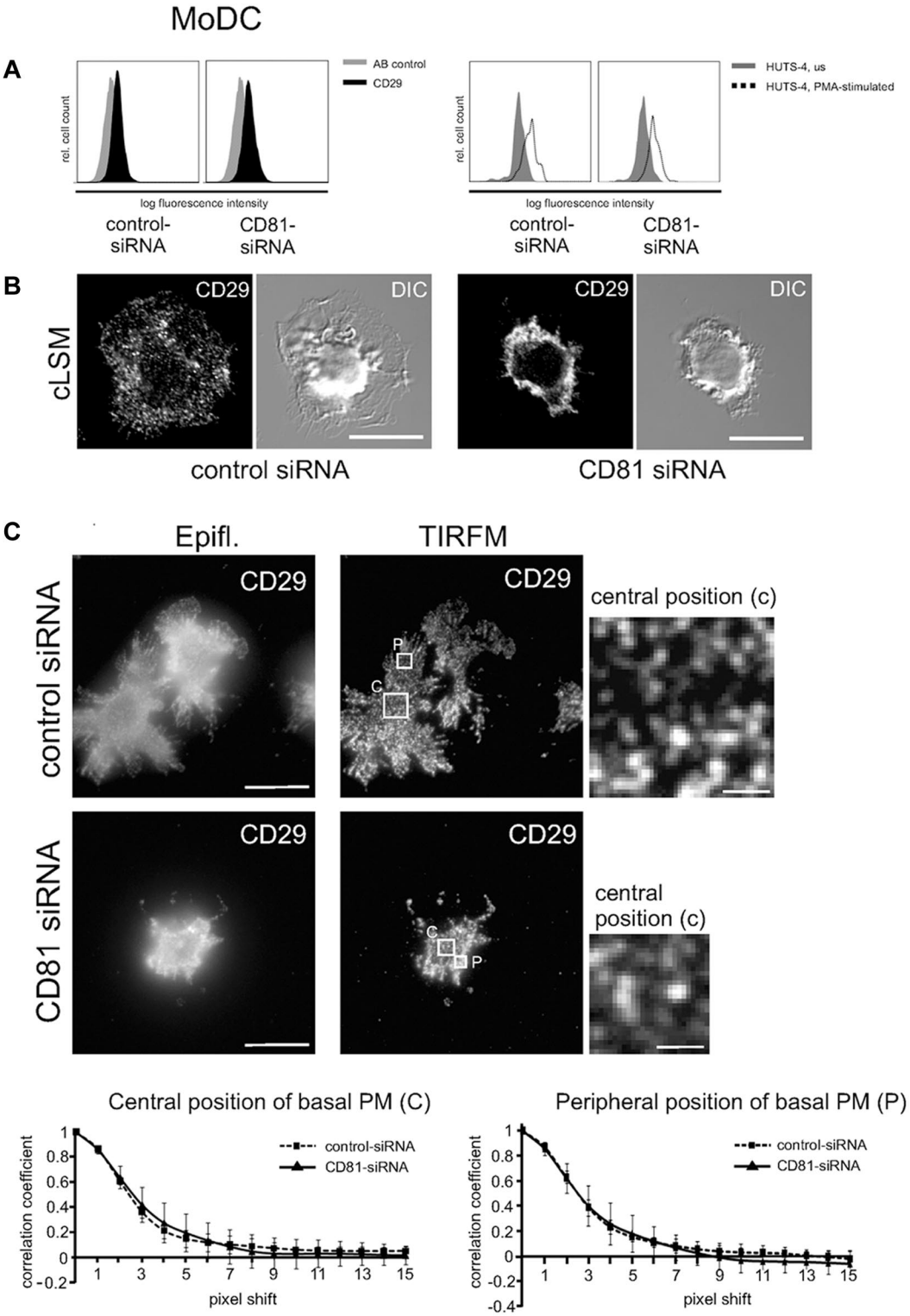

Figure 4. CD81 neither regulates β1-integrin affinity nor avidity, but it organizes integrin cluster distribution in DCs. (A) Flow cytometric analysis shows that a constitutive CD29 epitope is not altered after RNAi of CD81 (left panel). AB indicates antibody. Furthermore, β1 integrin affinity is not abrogated after RNAi of CD81, as shown by flow cytometry of a β1 integrin activation epitope detected by a monoclonal antibody HUTS-4 (right panel). (B) Immunofluorescence staining of β1 integrins (CD29) in LPS-stimulated CD81 RNAi knockdown Mo-DCs and control cells, respectively. The fluorescence staining images are confocal images (cLSM), focused to the basal plasma membrane of the respective cells. DIC indicates differential interference contrast. (C) Images generated with TIRF microscopy allow the visualization of individual CD29 clusters within the basal plasma membrane with high resolution. Individual CD29 cluster size was measured in central (c) as well as peripheral (p) positions of the basal plasma membrane (PM) with the help of autocorrelation analysis by the use of ImageJ software (bottom panel). The cells were adhered to 2-dimensional fibronectin-coated surfaces (5 μg/cm^2). Bars represent 10 and 1 μm (magnified detail), respectively. Epifl. means epifluorescence image of corresponding TIRFM Image (C).

We conclude from these findings that CD81 does not regulate β1 integrin avidity at the level of cluster size.

Immunofluorescence studies showed that CD81 is strongly colocalized with F-actin, Rac1, and integrins (both CD18 and

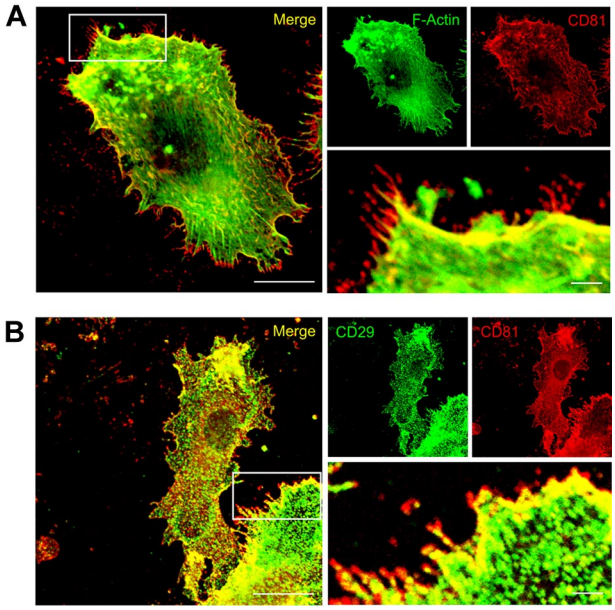

Figure 5. CD81 colocalizes with F-actin and CD29 at the leading edge of migration-relevant membrane protrusions. Immunofluorescence staining of CD81 (red fluorescence, A) and detection of F-Actin localization by the use of Alexa488-phalloidin (green fluorescence, A). Immunofluorescence staining of CD81 (red fluorescence, B) and beta1 integrins (CD29, green fluorescence, B) in LPS-stimulated Mo-DC. The cells were adhered to two-dimensional fibronectin-coated surfaces (5μg/cm^2). The fluorescence stainings are confocal images, focused on the basal plasma membrane of the cell. Bars represent 10 μm and 2 μm (magnified detail), respectively.

CD29) in migration-relevant membrane protrusions of LPS-stimulated wild-type DCs (Figures 3 and 5; supplemental Figure 2). Intriguingly, CD81 is also strongly expressed in front of the CD81/F-actin/β1-integrin areas of colocalization, that is, in the very front of the leading edges (Figures 3 and 5). From these data, we propose that CD81 organizes preformed adhesion structures at the leading edge of protruding lamellipodia.

CD81 regulates integrin-dependent adhesion and retrograde actin flow at the leading edge of migrating DCs

To investigate into a possible role of CD81 in adhesion structures and cytoskeletal dynamics at the leading edge of membrane protrusions, we transfected BM-DCs with Lifeact-EGFP, a recently described actin-binding peptide, that leaves actin dynamics unaffected and allows dynamic visualization of actin flow near the basal plasma membrane of the cells.[26] To observe the cells on exposure to polarizing CCL19, we used an assay system that allowed us to follow the morphologic response of BM-DCs by time-lapse videomicroscopy. Because LPS-stimulated BM-DCs are weakly adherent, we chose a setup where the cells are squeezed between an agarose gel and a fibronectin-coated surface. The spatial constraint in this setting, comparable with compacted 3-dimensional interstitial environments, causes flattening of polarized cells. We visualized cell migration, membrane dynamics, and cortical actin flow with time-lapse confocal microscopy and focused the objective on the basal plasma membrane. Actin cortical flow was analyzed by computer-assisted kymograph and line-scan analysis, using ImageJ (Figure 6; supplemental Video 5). Figure 6 shows that retrograde actin flow velocities at the leading edge of protruding membranes are increased from a mean of 1.88 μm/min (± 0.69 SD) in wild-type cells to 2.59 μm/min (± 0.7 SD) in *CD81*$^{-/-}$ BM-DC (Figure 6I). Furthermore, the quantitative changes in actin dynamics observed in *CD81*$^{-/-}$ BM-DCs were comparable to positive control cells that had been treated with Talin1 siRNA (Figure 6J). The knockdown of Talin1 results in an intracellular uncoupling of the linkage between all known integrins and the actin cytoskeleton.[35] Accordingly, increased retrograde actin flow in both *CD81*$^{-/-}$ and Talin1 RNAi knockdown BM-DCs provoked increased actin polymerization rates, because membrane protrusion speed was unaltered (supplemental Figure 3). Similar findings were described before for integrin-deficient DCs.[29] We therefore conclude from our results that increased retrograde actin flow in *CD81*$^{-/-}$ BM-DCs is caused by decreased integrin adhesion.

CD81 is not required for migration of DCs in complex 3-dimensional tissues in vitro

The quantification of cell migration within 3-dimensional ECM has become an important tool to investigate how cells integrate molecular events into higher order positioning within the tissue.[36] To simulate a complex fibrillar scaffold, we used 3D collagen type I gels and analyzed the migratory behavior of DCs in vitro. We have shown previously that chemotaxis of BM-DCs within collagen type I gels is excellently inducible with the chemokine CCL19 and that there are 2 different cell migration modes in these assays, 1 mode integrin dependent and 1 mode integrin independent.[20] Tracks of single cells visualized as plots show that in contrast to migration on 2-dimensional substrates (Figure 1B), chemotaxis of LPS-stimulated *CD81*$^{-/-}$ BM-DCs within a 3-dimensional matrix was not abrogated compared with wild-type cells (Figure 7A; supplemental Videos 6-7). We calculated that average velocity and y-forward migration index (Figure 7B-C) of *CD81*$^{-/-}$ BM-DCs were not significantly affected compared with wild-type cells. These results were confirmed by analyzing chemotaxis of CD81 RNAi knockdown BM-DCs in 3-dimensional collagen gels (supplemental Figure 4A-C) and under a compact agarose gel, which allows visualization of the morphology, and especially lamellipodia formation of motile cells in higher resolution (supplemental Figure 4D-F; supplemental Video 10). We conclude that CD81 is not required for DC migration in spatially restricted environments, for example, in 3-dimensional collagen gels or under agarose.

Rac1 activity is required for the formation of intact actin protrusions and DC migration in 3-dimensional collagen gels

Although the importance of the actin cytoskeleton and the small Rho GTPases in cell migration has been widely documented,[14,37] the specific functions of the different Rac isoforms in complex environments are still unclear. We therefore assessed BM-DC migration within 3-dimensional collagen gels after inactivation of the respective Rac protein by RNAi or by the use of a specific inhibitor. First, we performed qRT-PCR analysis to identify the mRNA levels of different Rac isoforms expressed in BM-DCs. These cells do not express Rac3, but both Rac1 and Rac2 are present, with an approximate expression ratio of 4:1 at the RNA level (supplemental Figure 5E). Both CCL19-induced BM-DC migration in 3-dimensional collagen and lamellipodia formation were strongly reduced after inhibition of Rac1 activity, whereas knockdown of Rac2 by RNAi did not affect BM-DC migration in 3 dimensions significantly (supplemental Figure 5A-D,F; and supplemental Videos 8-9).

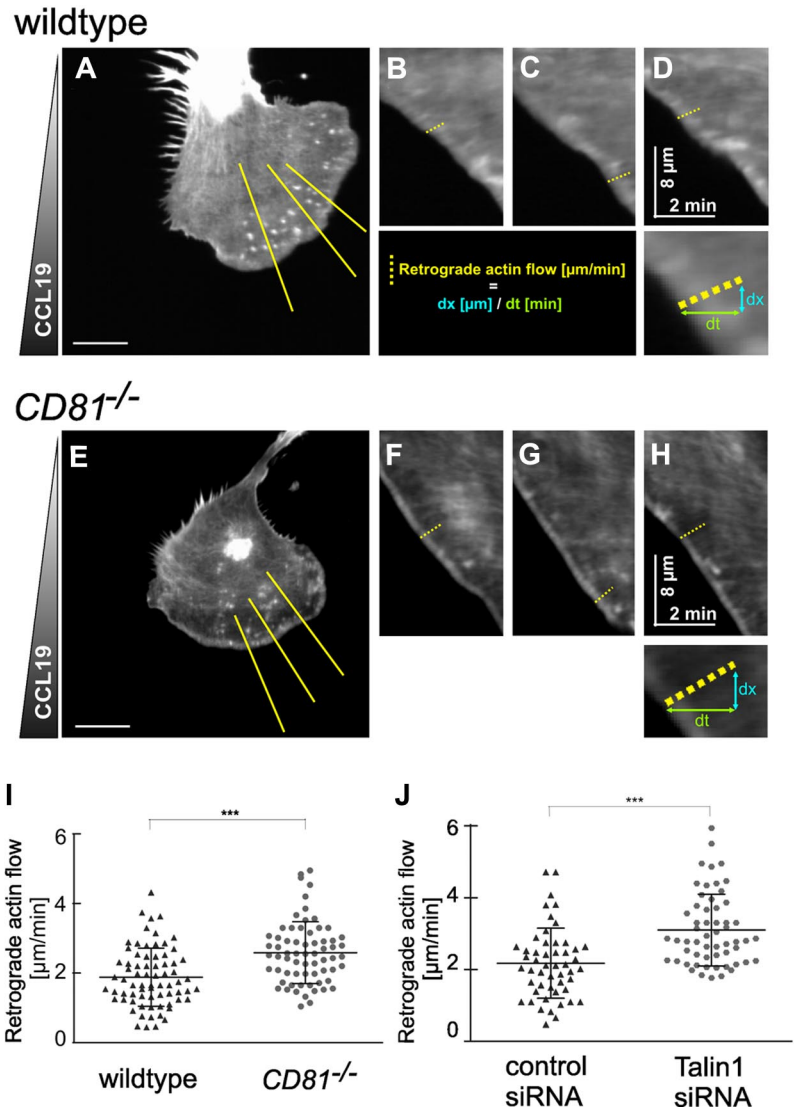

Figure 6. CD81 regulates integrin-dependent adhesion and retrograde actin flow at the cell front. Confocal microscopical analysis of actin cytoskeleton dynamics at the cell front of migrating LPS-stimulated wild-type (A-D) and *CD81*$^{-/-}$ BM-DCs (E-H) in a CCL19 gradient (600 ng/mL). To vizualize actin dynamics, cells were transfected with Lifeact-EGFP. Because of low adherence of mature BM-DCs, the cells were squeezed between an agarose gel and a fibronectin-coated surface, which represents a 3-dimensional environment. Actin dynamics and chemotaxis of motile cells were visualized at the basal plasma membrane by the use of a confocal microscope. BM-DCs were tracked over a period of 5 minutes at 2 seconds per frame. Retrograde actin flow was analyzed by kymograph analysis and line scan analysis (B-D,F-H) of yellow lines (in panels A and E, respectively) using ImageJ. (I) Quantification of retrograde actin flow velocities of migrating *CD81*$^{-/-}$ and wild-type BM-DCs, respectively. (J) Quantification of retrograde actin flow velocities of migrating Talin1 RNAi BM-DCs and control BM-DCs, respectively. Three kymographs per cell were analyzed; each dot represents the value of 1 single kymograph (I-J). Shown data are representative for 1 experiment of 3. Error bars indicate ± SD. ***$P \leq .001$. Bars represent 10 µm.

Discussion

Here, we demonstrate the requirement of CD81 for the formation of cell front actin protrusions during immune cell chemotaxis. CD81 is a member of the tetraspanin family that is capable of recruiting signaling enzymes, including protein kinase C,[3] known to be involved in phosphorylating integrins, or intracellular components of G protein-coupled receptors. Here, we show that CD81 acts upstream of integrins and Rac1 both in human and murine DCs. Consistently, we established CD81 as an important regulator of immune cell chemotaxis on 2-dimensional surfaces. In contrast, CD81 is not required for DC motility in 3-dimensional tissue-like environments, in which immune cells can migrate without integrins.[19] A recent study employed integrin-deficient BM-DCs in under-agarose assays, in which "cell slippage" in the absence of integrins is compensated by an enhancement in actin turnover, ie, by a simultaneous increase of actin polymerization and retrograde flow.[29] Thus, although there is no obvious integrin loss phenotype at the cell level during 3-dimensional migration of DCs, the absence of these molecules may still be detected at the molecular level. We conclude that the increase in retrograde actin flow in CD81-deficient BM-DCs indicates a functional compensation similar to that in integrin-deficient BM-DCs,[29] which further underscores the tight connection between CD81 and integrins.

Tetraspanins form clusters with several other cell surface proteins, including β1-integrins (in particular α_3/β_1, α_4/β_1, and α_6/β_1). This has led to the suggestion that they might play important roles as cell surface organizers,[6] or facilitators,[38] that interconnect other membrane proteins.[39] CD81 was shown to associate with the α_4/β_1 integrin, thereby strengthening B-cell adhesion under shear flow conditions[9] or regulating endothelial

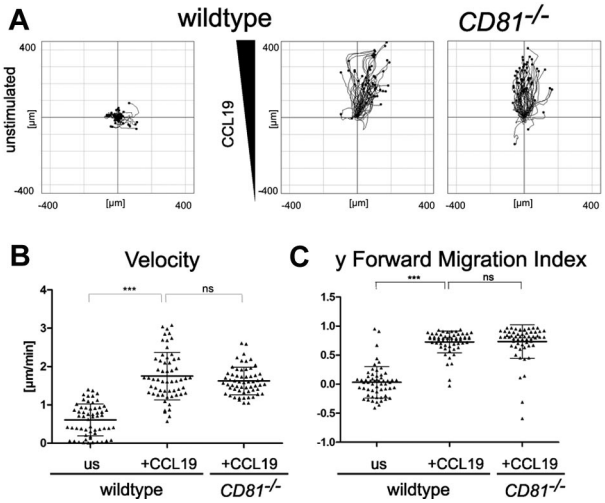

Figure 7. CD81 is not required for CCL19-induced BM-DC chemotaxis in 3-dimensional collagen gels. Chemotactic migration of BM-DCs from *CD81*$^{-/-}$ and wild-type mice in 3-dimensional collagen type I gels (1.6 μg/mL) in response to a stable CCL19 gradient (600 ng/mL). (A) Migration plots of 60 cells/sample monitored by time-lapse videomicroscopy over a period of 3 hours by capturing digital images every 5 minutes. Quantification of average migratory speed (velocity; B) and y-forward migration index (y-FMI, which means directional persistence toward the chemokine; C) of migrating BM-DCs after manual tracking of motile cells. Results are representative for 1 experiment of 3. Error bars indicate ± SD. ns, not significant. ***$P \leq .001$.

lateral junctions.[40] Our results now substantially extend this notion in showing that CD81 is essential for integrin-dependent but not for integrin-independent DC chemotaxis, which highlights a fundamental role of the molecule as a functional regulator of integrins in the formation of adhesion-dependent protrusions.

How does CD81 organize integrin dependent Rac-activation in immune cell migration? Integrins need to be activated to engage extracellular components. These ligands may either be a variety of different matrix proteins or cell surface molecules, and both classes of interactors can direct cell motility. The integrin activation process is still not fully understood but involves both conformational changes that are regulated by cytoplasmic signaling factors or components of the actin cytoskeleton, for example, talin, the kindlins, Rap1, or the cytohesins. Ligand-bound integrins engage in multiple intracellular signaling events that result in, eg, adhesion strengthening and F-actin-dependent cell shape changes (reviewed in[41-43]). The activation of Rho GTPases is of central importance for this function,[34] and we consistently detected a selective loss of Rac1 activity in CD81-deficient DCs. Interestingly, Brazzoli et al[44] found earlier that engagement of CD81 regulates hepatitis C virus infection in human hepatocytes via activation of Rho GTPases. We found that both CD81 and Rac1 are mobilized to the cell front in an adhesion-dependent manner, and the loss of lamellipodia formation in CD81$^{-/-}$ cells is in full concordance with these observations. Importantly, because Rac1 was found to be required for DC migration in 3 dimensions, a direct signaling link of CD81 to Rac is unlikely. It needs to be stated, however, that it is currently unclear how Rac is regulated in the 3-dimensional setting, ie, in the absence of CD81 or integrins.

Importantly, we could not establish a role of CD81 in the conformational regulation of β1 integrins, because the generation of a specific activation epitope was found unaltered in CD81-deficient cells. This is in line with previous findings on the role of CD81 in extravasation.[9] However, we observed by the use of both epifluorescence and confocal imaging an apparent accumulation of integrin clusters in cells lacking CD81 compared with wild-type cells. On close analysis using TIRF microscopy, in which only the basal cell layer is illuminated, we were surprised to find almost identical integrin cluster sizes and distributions in the respective contact areas of both wild-type and CD81-deficient cells. The accumulation of anti-integrin fluorescence had thus occurred in apical and lateral plasma membrane regions, in which the adhesion receptors are therefore not engaged with ligands and cannot contribute to adhesion strengthening and Rac signaling. CD81, β1-integrins, β2-integrins, and Rac1 are strongly colocalized at the leading edge of adherent DCs. However, and most strikingly, we discovered CD81-containing structures at the very front of these cells, which even protrudes from F-actin or from the leading edge β1-integrins. We therefore propose that CD81 might be required for the mobilization of preformed integrin clusters into these front membranes, and future studies will have to address the precise underlying mechanisms in detail. Signaling might play a role, but biophysical mechanisms of cell surface protein cluster dynamics regulation[45,46] might contribute significantly to the observed phenomena, too.

Acknowledgments

The authors thank Peter Lipp for providing Lifeact-EGFP. They also thank Elke Thome for technical assistance, and members of the laboratory of Molecular Immunology for discussion and comments on the manuscript.

This work was supported by the Deutsche Forschungsgemeinschaft (SFBs 645 and 704). F.E. is a scholar of the NRW International Graduate Research School, LIMES Chemical Biology.

Authorship

Contribution: W.K. designed the study, wrote the manuscript, and acquired research funding; T.Q. designed and performed research and wrote the manuscript; F.E. performed research, analyzed data, and discussed results; V.S., Y.H., and C.S. performed research and analyzed data; S.L. contributed tools and discussed results; and T.L. and C.K. discussed results.

Conflict-of-interest disclosure: The authors declare no competing financial interests.

Correspondence: Waldemar Kolanus, LIMES Institute, Carl-Troll-Straße 31, D-53115 Bonn, Germany; e-mail: wkolanus@ uni-bonn.de.

References

1. Hemler ME. Targeting of tetraspanin proteins–potential benefits and strategies. *Nat Rev Drug Discov.* 2008;7(9):747-758.
2. Hemler ME, Mannion BA, Berditchevski F. Association of TM4SF proteins with integrins: relevance to cancer. *Biochim Biophys Acta.* 1996; 1287(2-3):67-71.
3. Zhang XA, Bontrager AL, Hemler ME. Transmembrane-4 superfamily proteins associate with activated protein kinase C (PKC) and link PKC to specific beta(1) integrins. *J Biol Chem.* 2001; 276(27):25005-25013.
4. Hemler ME. Tetraspanin proteins mediate cellular penetration, invasion, and fusion events and define a novel type of membrane microdomain. *Annu Rev Cell Dev Biol.* 2003;19:397-422.
5. Levy S, Shoham T. The tetraspanin web modulates immune-signalling complexes. *Nat Rev Immunol.* 2005;5(2):136-148.
6. Rubinstein E, Ziyyat A, Prenant M, et al. Reduced

fertility of female mice lacking CD81. *Dev Biol.* 2006;290(2):351-358.

7. Maecker HT, Levy S. Normal lymphocyte development but delayed humoral immune response in CD81-null mice. *J Exp Med.* 1997;185(8):1505-1510.
8. Shoham T, Rajapaksa R, Kuo CC, Haimovich J, Levy S. Building of the tetraspanin web: distinct structural domains of CD81 function in different cellular compartments. *Mol Cell Biol.* 2006;26(4):1373-1385.
9. Feigelson SW, Grabovsky V, Shamri R, Levy S, Alon R. The CD81 tetraspanin facilitates instantaneous leukocyte VLA-4 adhesion strengthening to vascular cell adhesion molecule 1 (VCAM-1) under shear flow. *J Biol Chem.* 2003;278(51):51203-51212.
10. Coffey GP, Rajapaksa R, Liu R, et al. Engagement of CD81 induces ezrin tyrosine phosphorylation and its cellular redistribution with filamentous actin. *J Cell Sci.* 2009;122(Pt 17):3137-3144.
11. Mittelbrunn M, Yanez-Mo M, Sancho D, Ursa A, Sanchez-Madrid F. Cutting edge: dynamic redistribution of tetraspanin CD81 at the central zone of the immune synapse in both T lymphocytes and APC. *J Immunol.* 2002;169(12):6691-6695.
12. Garcia E, Pion M, Pelchen-Matthews A, et al. HIV-1 trafficking to the dendritic cell-T-cell infectious synapse uses a pathway of tetraspanin sorting to the immunological synapse. *Traffic.* 2005;6(6):488-501.
13. Cocquerel L, Voisset C, Dubuisson J. Hepatitis C virus entry: potential receptors and their biological functions. *J Gen Virol.* 2006;87(Pt 5):1075-1084.
14. Ridley AJ, Schwartz MA, Burridge K, et al. Cell migration: integrating signals from front to back. *Science.* 2003;302(5651):1704-1709.
15. Friedl P, Gunzer M. Interaction of T cells with APCs: the serial encounter model. *Trends Immunol.* 2001;22(4):187-191.
16. Friedl P, Brocker EB. T cell migration in three-dimensional extracellular matrix: guidance by polarity and sensations. *Dev Immunol.* 2000;7(2-4):249-266.
17. Friedl P, Entschladen F, Conrad C, Niggemann B, Zanker KS. CD4+ T lymphocytes migrating in three-dimensional collagen lattices lack focal adhesions and utilize beta1 integrin-independent strategies for polarization, interaction with collagen fibers and locomotion. *Eur J Immunol.* 1998;28(8):2331-2343.
18. Werr J, Xie X, Hedqvist P, Ruoslahti E, Lindbom L. beta1 integrins are critically involved in neutrophil locomotion in extravascular tissue in vivo. *J Exp Med.* 1998;187(12):2091-2096.
19. Lämmermann T, Bader BL, Monkley SJ, et al. Rapid leukocyte migration by integrin-independent flowing and squeezing. *Nature.* 2008;453(7191):51-55.
20. Quast T, Tappertzhofen B, Schild C, et al. Cytohesin-1 controls the activation of RhoA and modulates integrin-dependent adhesion and migration of dendritic cells. *Blood.* 2009;113(23):5801-5810.
21. Friedl P, Brocker EB, Zanker KS. Integrins, cell matrix interactions and cell migration strategies: fundamental differences in leukocytes and tumor cells. *Cell Adhes Commun.* 1998;6(2-3):225-236.
22. Pollard TD, Borisy GG. Cellular motility driven by assembly and disassembly of actin filaments. *Cell.* 2003;112(4):453-465.
23. Heasman SJ, Ridley AJ. Mammalian Rho GTPases: new insights into their functions from in vivo studies. *Nat Rev Mol Cell Biol.* 2008;9(9):690-701.
24. Nattermann J, Zimmermann H, Iwan A, et al. Hepatitis C virus E2 and CD81 interaction may be associated with altered trafficking of dendritic cells in chronic hepatitis C. *Hepatology.* 2006;44(4):945-954.
25. Krämer B, Schulte D, Korner C, et al. Regulation of NK cell trafficking by CD81. *Eur J Immunol.* 2009;39(12):3447-3458.
26. Riedl J, Crevenna AH, Kessenbrock K, et al. Lifeact: a versatile marker to visualize F-actin. *Nat Methods.* 2008;5(7):605-607.
27. Friedl P, Storim J. Diversity in immune-cell interactions: states and functions of the immunological synapse. *Trends Cell Biol.* 2004;14(10):557-567.
28. Heit B, Kubes P. Measuring chemotaxis and chemokinesis: the under-agarose cell migration assay. *Sci STKE.* 2003;2003(170):PL5.
29. Renkawitz J, Schumann K, Weber M, et al. Adaptive force transmission in amoeboid cell migration. *Nat Cell Biol.* 2009;11(12):1438-1443.
30. Okamura Y, Schmidt R, Raschke I, et al. A few immobilized thrombins are sufficient for platelet spreading. *Biophys J.* 2011;100(8):1855-1863.
31. Förster R, Davalos-Misslitz AC, Rot A. CCR7 and its ligands: balancing immunity and tolerance. *Nat Rev Immunol.* 2008;8(5):362-371.
32. Yang X, Kovalenko OV, Tang W, Claas C, Stipp CS, Hemler ME. Palmitoylation supports assembly and function of integrin-tetraspanin complexes. *J Cell Biol.* 2004;167(6):1231-1240.
33. Small JV, Auinger S, Nemethova M, et al. Unravelling the structure of the lamellipodium. *J Microsc.* 2008;231(3):479-485.
34. Ridley AJ. Rho GTPases and actin dynamics in membrane protrusions and vesicle trafficking. *Trends Cell Biol.* 2006;16(10):522-529.
35. Critchley DR. Genetic, biochemical and structural approaches to talin function. *Biochem Soc Trans.* 2005;33(Pt 6):1308-1312.
36. Friedl P, Brocker EB. Reconstructing leukocyte migration in 3D extracellular matrix by time-lapse videomicroscopy and computer-assisted tracking. *Methods Mol Biol.* 2004;239:77-90.
37. Burridge K, Wennerberg K. Rho and Rac take center stage. *Cell.* 2004;116(2):167-179.
38. Maecker HT, Todd SC, Levy S. The tetraspanin superfamily: molecular facilitators. *FASEB J.* 1997;11(6):428-442.
39. Horváth G, Serru V, Clay D, Billard M, Boucheix C, Rubinstein E. CD19 is linked to the integrin-associated tetraspans CD9, CD81, and CD82. *J Biol Chem.* 1998;273(46):30537-30543.
40. Yáñez-Mó M, Alfranca A, Cabanas C, et al. Regulation of endothelial cell motility by complexes of tetraspan molecules CD81/TAPA-1 and CD151/PETA-3 with alpha3 beta1 integrin localized at endothelial lateral junctions. *J Cell Biol.* 1998;141(3):791-804.
41. Laudanna C, Bolomini-Vittori M. Integrin activation in the immune system. *Wiley Interdiscip Rev Syst Biol Med.* 2009;1(1):116-127.
42. Ley K, Laudanna C, Cybulsky MI, Nourshargh S. Getting to the site of inflammation: the leukocyte adhesion cascade updated. *Nat Rev Immunol.* 2007;7(9):678-689.
43. Alon R. Chemokine arrest signals to leukocyte integrins trigger bi-directional-occupancy of individual heterodimers by extracellular and cytoplasmic ligands. *Cell Adh Migr.* 2010;4(2):211-214.
44. Brazzoli M, Bianchi A, Filippini S, et al. CD81 is a central regulator of cellular events required for hepatitis C virus infection of human hepatocytes. *J Virol.* 2008;82(17):8316-8329.
45. Sieber JJ, Willig KI, Kutzner C, et al. Anatomy and dynamics of a supramolecular membrane protein cluster. *Science.* 2007;317(5841):1072-1076.
46. Yang J, Reth M. Oligomeric organization of the B-cell antigen receptor on resting cells. *Nature.* 2010;467(7314):465-469.